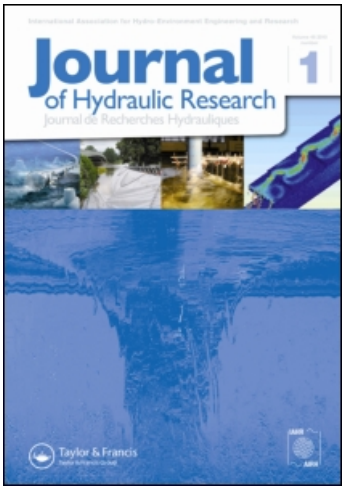

Journal of Hydraulic Research
Publication details, including instructions for authors and subscription information:
http://www.informaworld.com/smpp/title~content=t916282780

Physically-consistent wall boundary conditions for the k-ω turbulence model

David R. Fuhrman[a]; Martin Dixen[b]; Niels Gjøl Jacobsen[a]
[a] Department of Mechanical Engineering, Technical University of Denmark, Lyngby, Denmark [b] Port and Offshore Technology, Hørsholm, Denmark

Online publication date: 13 December 2010

To cite this Article Fuhrman, David R. , Dixen, Martin and Jacobsen, Niels Gjøl(2010) 'Physically-consistent wall boundary conditions for the k-ω turbulence model', Journal of Hydraulic Research, 48: 6, 793 — 800
To link to this Article: DOI: 10.1080/00221686.2010.531100
URL: http://dx.doi.org/10.1080/00221686.2010.531100

IAHR AIRH
Taylor & Francis
Taylor & Francis Group

Journal of Hydraulic Research Vol. 48, No. 6 (2010), pp. 793–800
doi:10.1080/00221686.2010.531100

Research paper

Physically-consistent wall boundary conditions for the k-ω turbulence model

DAVID R. FUHRMAN, Associate Professor, *Department of Mechanical Engineering, Technical University of Denmark, Nils Koppels Allé, Building 403, DK-2800 Kgs. Lyngby, Denmark.*
Email: drf@mek.dtu.dk (author for correspondence)

MARTIN DIXEN, *DHI, Port and Offshore Technology, Agern Allé 5, DK-2970 Hørsholm, Denmark.*
Email: mdi@dhigroup.com

NIELS GJØL JACOBSEN, PhD Student, *Department of Mechanical Engineering, Technical University of Denmark, Nils Koppels Allé, Building 403, DK-2800 Kgs. Lyngby, Denmark.*
Email: ngj@mek.dtu.dk

ABSTRACT
A model solving Reynolds-averaged Navier–Stokes equations, coupled with k-ω turbulence closure, is used to simulate steady channel flow on both hydraulically smooth and rough beds. Novel experimental data are used as model validation, with k measured directly from all three components of the fluctuating velocity signal. Both conventional $k = 0$ and $\mathrm{d}k/\mathrm{d}y = 0$ wall boundary conditions are considered. Results indicate that either condition can provide accurate solutions, for the bulk of the flow, over both smooth and rough beds. It is argued that the zero-gradient condition is more consistent with the near wall physics, however, as it allows direct integration through a viscous sublayer near smooth walls, while avoiding a viscous sublayer near rough walls. This is in contrast to the conventional $k = 0$ wall boundary condition, which forces resolution of a viscous sublayer in all circumstances. Subsequent testing demonstrates that the zero-gradient condition allows the near-bed grid spacing near rough walls to be based on the roughness length, rather than the conventional viscous length scale, hence offering significant computational advantages.

Keywords: Boundary conditions, hydraulic roughness, k-ω model, turbulence, turbulence modelling

1 Introduction

Among the most popular two-equation turbulence closures for the Reynolds-averaged Navier–Stokes (RANS) equations is the k-ω model, where k is the specific turbulent kinetic energy and ω the specific dissipation rate. The k-ω model has evolved over the past six decades (e.g. Wilcox 2006, 2008, and references therein) and is particularly well known for its superior performance over the k-ε model for boundary layers with adverse pressure gradients. It has been successfully used to simulate a wide range of flows (e.g. numerous examples of Wilcox 2006) and is highly popular with both scientists and engineers.

An additional key advantage of k-ω formulations is that effects of wall roughness can be imposed directly via the ω boundary condition, which is traditionally expressed as a scaled function of the roughness Reynolds number $k_N{}^+ = k_N U_f/\nu$, where k_N is Nikuradse's equivalent sand grain roughness, U_f the friction velocity, and ν the fluid kinematic viscosity. Within this context, the conventional practice is to treat all walls (i.e. hydraulically smooth or rough) similarly, using a strict no-slip condition whereby all mean velocity components u_i, as well as the turbulent kinetic energy k, are set to zero at a wall boundary. This is fundamentally sound for hydraulically smooth conditions, as the model then allows a direct integration through the viscous sublayer, consistent with the underlying near-wall physics.

This strategy can create notorious numerical difficulties for large roughness simulations, however (e.g. Patel and Yoon 1995, Patel 1998, Knopp *et al.* 2009). Setting $k = 0$ at a hydraulically rough wall forces a viscous sublayer to be present in the model domain, contradicting the notion that this layer is disrupted completely under "fully rough" conditions. Consequently, the conventional strategy requires near-wall grid spacing Δy to be based on the viscous length scale ν/U_f, commonly requiring $\Delta y^+ = \Delta y U_f/\nu < 1$, rather than the more natural roughness length k_N. Put another way, a forced viscous sub-layer

Revision received 7 October 2010/Open for discussion until 30 June 2011.

ISSN 0022-1686 print/ISSN 1814-2079 online
http://www.informaworld.com

inconveniently requires computational grids to be Reynolds number-dependent, even under hydraulically rough conditions, where the underlying physics largely are not. In practice, this requires the use of highly-stretched grids, resulting in increased computational burden.

With this problem in mind, the present research aims to explore the advantages of a physically sound, but under-utilized, strategy for posing boundary conditions at friction walls within the context of k-ω simulations, being simply that of a zero normal gradient for k. Novel experimental data within steady open-channel flows on both smooth and rough beds are presented, where the k-profile is measured directly from all three fluctuating velocity components. These test conditions are simulated utilizing both $k = 0$ and $\mathrm{d}k/\mathrm{d}y = 0$ wall boundary conditions. It will be demonstrated that results using a zero-gradient condition are generally similar for the bulk of the flow to those using the conventional $k = 0$ approach, for both smooth and rough beds, while offering potentially significant computational advantages for rough beds in terms of the required near wall resolution.

2 Experimental description

Experiments involving steady, uniform, open-channel flow have been performed at the hydraulics laboratory, Technical University of Denmark. These were performed in a 10 m long, 0.30 m wide, and 0.30 m high tilting flume. The water temperature was within 20.6–21.0°C, from which $\nu = 9.6 \times 10^{-7}\,\mathrm{m}^2/\mathrm{s}$. Velocity measurements were made with a DANTEC two-component Laser Doppler Anemometer (LDA) equipped with a DANTEC 55N12 frequency shifter, a DANTEC 55N21 frequency tracker, and a 300 mW argon-ion laser.

Flows on both hydraulically smooth and rough beds were considered, where all three velocity components, and therefore the turbulent kinetic energy $k = (1/2)u_i'u_i'$, where u_i' are Cartesian fluctuating velocity components, have been directly measured over the depth. For the smooth bed, the bottom consisted of Plexiglas, and the measured flow depth from the base to the free surface was $h = 60$ mm. The measurement section was located at the tilting flume axis, 5 m from the flume inlet. The streamwise (horizontal) and vertical velocity components were first measured using the two-component LDA mounted from the channel side, whereas the transverse component was measured with the LDA mounted on top of the channel, such that the laser shot through the smooth free surface. For each measurement, the total sampling time was 180 s, with a measurement frequency of 90 Hz. Based on a standard log-fit using the measured mean (discrete time-averaged) horizontal velocity profile $u(y)$ over the logarithmic region $30 < y^+ = yU_f/\nu < 0.2hU_f/\nu = 200$, the friction velocity was estimated to be $U_f = 0.016$ m/s for a Reynolds number $\mathsf{R} = Vh/\nu = 1.9 \times 10^4$, with $V = 0.31$ m/s the mean velocity over the depth. The root-mean-squared error (RMSE) for the measured u/U_f relative to the analytical logarithmic profile within the region specified above was found to be 0.10 (see Fig. 2a).

In the rough bed case, a single layer of pebble-sized stones was placed on the channel base, of median diameter $d = 7$ mm. The free surface was measured to be 67 mm above the channel base. The reported measured quantities result from a spatial averaging of three separate profiles measured at different plan positions over a single stone located near the channel centre (Dixen *et al.* 2007). Based on a log-fit of the resulting mean (spatially averaged) velocity profile, now over the range $0.5 < y/k_N < 0.2h/k_N = 1.25$ (see Fig. 3a), the friction velocity was estimated to be $U_f = 0.021$ m/s, with $k_N = 9.9$ mm, and the theoretical bottom lying $0.29d$ below the top of the stones. The RMSE for the measured u/U_f values relative to the analytical logarithmic profile within the region specified above was found to be 0.032. These values result in a flow depth from the theoretical bottom to the free surface of $h = 62.0$ mm, with mean velocity $V = 0.22$ m/s. In terms of non-dimensional quantities $\mathsf{R} = 1.4 \times 10^4$, with roughness Reynolds number $k_N{}^+ = 200$. As $k_N{}^+ > 70$, the conditions may indeed be regarded as fully rough.

Such experimental measurements, for flow over rough beds in particular, are fairly scarce. The present tests are novel, in that the vertical profile for the turbulent kinetic energy k was directly measured from all three fluctuating velocity components. Hence, they are a valuable physical realization of turbulence characteristics near a rough wall, in addition to serving as a reference for turbulence models, as shown below.

3 Model description

The numerical model considered solves the incompressible RANS and continuity equations, namely

$$\frac{\partial u_i}{\partial t} + u_j\frac{\partial u_i}{\partial x_j} = -\frac{1}{\rho}\frac{\partial p}{\partial x_j} + \frac{\partial}{\partial x_j}\left(2\nu S_{ji} - \tau_{ij}\right) \tag{1}$$

$$\frac{\partial u_i}{\partial x_i} = 0 \tag{2}$$

where the Reynolds stress tensor τ_{ij} is expressed in terms of an eddy viscosity ν_T as

$$\tau_{ij} = 2\nu_T S_{ij} - \frac{2}{3}k\delta_{ij}, \quad S_{ij} = \frac{1}{2}\left(\frac{\partial u_i}{\partial x_j} + \frac{\partial u_j}{\partial x_i}\right) \tag{3}$$

where δ_{ij} is the Kronecker delta. To close the system, the k–ω turbulence model proposed by Wilcox (2006, 2008) is adapted. This model defines the kinematic eddy viscosity as

$$\nu_T = \frac{k}{\tilde{\omega}}, \quad \tilde{\omega} = \max\left\{\omega, C_{\lim}\sqrt{\frac{2S_{ij}S_{ij}}{\beta^*}}\right\} \tag{4}$$

The model uses transport equations for specific turbulent kinetic energy k and specific dissipation rate ω

$$\frac{\partial k}{\partial t} + u_j \frac{\partial k}{\partial x_j} = \tau_{ij} \frac{\partial u_i}{\partial x_j} - \beta^* k\omega + \frac{\partial}{\partial x_j}\left[\left(\nu + \sigma^* \frac{k}{\omega}\right)\frac{\partial k}{\partial x_j}\right] \quad (5)$$

$$\frac{\partial \omega}{\partial t} + u_j \frac{\partial \omega}{\partial x_j} = \alpha \frac{\omega}{k} \tau_{ij} \frac{\partial u_i}{\partial x_j} - \beta\omega^2 + \frac{\sigma_d}{\omega} \frac{\partial k}{\partial x_j} \frac{\partial \omega}{\partial x_j} + \frac{\partial}{\partial x_j}\left[\left(\nu + \sigma \frac{k}{\omega}\right)\frac{\partial \omega}{\partial x_j}\right] \quad (6)$$

where $\sigma_d = H\{\partial k/\partial x_j \cdot \partial\omega/\partial x_j\}\sigma_{do}$, and $H\{\bullet\}$ is the Heaviside step function, taking a value of unity if the argument is positive, and 0 otherwise. The standard closure coefficients suggested by Wilcox (2006) are: $C_{\lim} = 0.875$, $\alpha = 0.52$, $\beta = 0.0708$, $\beta^* = 0.09$, $\sigma = 0.5$, $\sigma^* = 0.6$, and $\sigma_{do} = 0.125$.

For the ω wall boundary condition the standard format of Wilcox (2006) is utilized:

$$\omega = \frac{U_f^2}{\nu} S_R, \quad y = 0 \quad (7)$$

$$S_R = \begin{cases} \left(\dfrac{200}{k_N^+}\right)^2, & k_N^+ \le 5 \\ \dfrac{K_r}{k_N^+} + \left[\left(\dfrac{200}{k_N^+}\right)^2 - \dfrac{K_r}{k_N^+}\right] e^{5-k_N^+}, & k_N^+ > 5 \end{cases} \quad (8)$$

where ${k_N}^+ = k_N U_f/\nu$ is the roughness Reynolds number, with U_f the friction velocity. Note that for large ${k_N}^+$ Eq. (8) tends to $S_R = K_r/{k_N}^+$, whereby Eq. (7) becomes $\omega = K_r U_f/k_N$, i.e. ω at the wall is independent of ν. Wilcox (2006) suggests setting $K_r = 100$, though this coefficient will be adjusted below.

The above equations are solved numerically using the open-source CFD toolbox OpenFOAM®[1] (version 1.5), making use of a second-order finite-volume spatial discretization, combined with a forward-Euler time-stepping scheme. Throughout the present work, only a single (vertical) spatial direction is considered, with the number of geometrically-stretched computational cells fixed at 100, though the implementation is more general. For steady-flow conditions, the horizontal pressure gradient is specified as a constant based on the desired friction velocity: $-(1/\rho)\,\partial p/\partial x = U_f^2/h$, where h is the total height of the model domain, taken to match the desired flow depth. The model is then run starting from motionless initial conditions until a steady state is reached. In all simulations considered, the top boundary is modelled as a frictionless rigid lid, where the vertical velocity is zero, and where gradients of all scalar quantities (and non-normal velocity components) are set to zero. At the bottom (friction wall) boundary, all mean velocity components u_i are set to zero.

Regarding the k wall boundary condition, two variants are considered. The first utilizes the traditional practice of setting $k = 0$ at the wall (e.g. Patel and Yoon 1995, Fuhrman *et al.* 2009, Knopp *et al.* 2009, Sana *et al.* 2009). When using this option, it was found that some important modifications are necessary for modelling flows on hydraulically rough surfaces with the present formulation. First, it was noticed that the stress limiting feature (i.e. the term proportional to $C_{\lim}$) in Eq. (4) can become active near a rough bed, resulting in strong Reynolds number dependence of the results, which is obviously undesirable. This problem with the Wilcox (2006) k-ω formulation has, to our knowledge, gone unrecognized. A similar problem has, however, been previously identified by Hellsten and Laine (1998) for the stress-limiting feature of the k-ω-SST turbulence model of Menter (1994), which was solved by adding an additional blending function. As the stress-limiting feature is not of principal interest herein, it is simply switched off by setting $C_{\lim} = 0$ when the $k = 0$ boundary condition is used, whereby Eq. (4) simplifies to the traditional $\nu_T = k/\omega$. Additionally, the rough wall constant in Eq. (8) was modified slightly from $K_r = 100$ to $K_r = 80$, which was necessary to bring computed hydraulically rough velocity profiles in-line with the standard law of the wall solutions. Regarding this issue, the computed velocity profiles shown in Fig. 4.24 of Wilcox (2006), based on $K_r = 100$, do not match the claimed law of the wall in his Eq. (4.197), consistent with our findings.

The second model variant will alternatively use a zero normal-gradient boundary condition for k, i.e. $\mathrm{d}k/\mathrm{d}y = 0$ at $y = 0$ for the present purposes. This strategy necessitates an additional modification in the rough wall coefficient in Eq. (8) to $K_r = 180$, which similarly brings computed velocity profiles for steady rough turbulent flows in-line with standard law of the wall solutions. While not standard practice, a zero-gradient k boundary condition was used previously by Roulund *et al.* (2005) in combination with a k-ω-SST turbulence model, though the numerical advantages were not there specifically explored. They also found that slight modifications to the S_R function were necessary when using this strategy. It is stressed that if the zero-gradient model variant is used the stress limiter is formally left on, i.e. $C_{\lim} = 0.875$, as originally described, though it does not apparently become active if this strategy is used.

The use of a zero-gradient wall boundary condition for k, rather than the conventionally used $k = 0$ boundary condition, is justifiable from physical considerations. As discussed, setting $k = 0$, and hence $\nu_T = 0$, at a rough wall forces a fictitious viscous sublayer (i.e. a region where $\nu > \nu_T$) to be present within the computational domain, which presents inconsistencies with the physics near a rough wall. For example, data collected by Bayazit (1976, 1983; also see e.g. Blinco and Partheniades 1971, Kamphuis 1974) indicate that for steady boundary layers the theoretical wall (here taken as $y = 0$) for rough beds corresponds to a location approximately (0.15–0.35)d below the top of the roughness elements, where d is the physical roughness height. This was further confirmed by recent research involving both ripple (e.g. Fredsøe *et al.* 1999) and stone (Sumer *et al.* 2001) bed roughness. This situation is shown in Fig. 1, where the $y = 0$ boundary, here placed $0.25d$

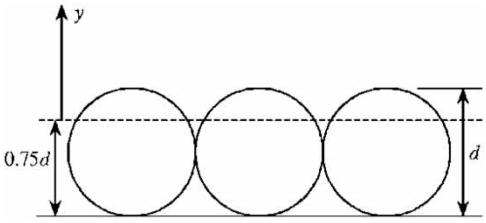

Figure 1 Conceptual sketch showing typical position of (– – –) the theoretical wall within uniformly placed roughness elements of diameter d

below the top of the roughness elements, would typically correspond to a position where pore space exists between grains, which could in principle be freely penetrated by turbulent kinetic energy, e.g. via small-scale flow separation and resulting vortex shedding around the roughness elements. While obviously such inter-granular details at a rough wall are only described in a bulk fashion within RANS-based models, a condition allowing, but not necessarily requiring, finite k at a wall-boundary would seem more consistent with the underlying rough-wall physics than the convention of simply taking $k = 0$. More specifically, a zero-gradient condition for k can be interpreted physically as specifying a zero flux of turbulent kinetic energy normal to a wall. This condition should in fact hold quite generally, as a wall (be it rough or smooth) is neither a direct source nor a sink of turbulent kinetic energy.

The zero-gradient condition is also generally supported by available measurements for steady flows near hydraulically rough beds. Experiments of Nezu (1977) and Sumer *et al.* (2003) show nearly uniform values of the mean turbulent kinetic energy profiles, based on a single horizontal fluctuating velocity component as a rough bed is approached. Note that their rough bed was composed largely of bed forms. This trend will also be apparent in the rough bed measurements described above of k for steady conditions, provided below.

4 Model results

Model comparisons against the previously described hydraulically smooth and rough bed experiments involving steady channel flow are now made. The comparison for the smooth bed case is presented in Fig. 2, where a good agreement between the measured and computed velocity profiles is observed. Both results follow closely the appropriate law of the wall solution, illustrating the logarithmic fit discussed in Section 2. The comparison for the turbulent kinetic energy profile, however, is less impressive, with the model under-predicting k near the bed (Fig. 2c). This is an established shortcoming of the k-ω model in hydraulically smooth conditions (Wilcox 2006, Figs. 4.28 and 4.29) for smooth channel and pipe flows. Note that the results shown in Fig. 2 use the $\mathrm{d}k/\mathrm{d}y = 0$ wall boundary condition, though the results for hydraulically smooth conditions are visually indistinguishable if either boundary condition (i.e. $k = 0$ or $\mathrm{d}k/\mathrm{d}y = 0$) is utilized, hence only the single result is shown here. This is again consistent with physical expectations, as there can be no flux of turbulent kinetic energy through a wall, i.e. both conditions are expectedly satisfied at a smooth wall, see model results in Fig. 2(c), upper right corner. Hence, while it is conventional to use $k = 0$ as a boundary condition on smooth beds, a zero-gradient condition is equally appropriate, and both conditions allow the integration through the viscous sublayer.

Similar comparisons are made for the hydraulically rough case in Fig. 3 for $k = 0$ and in Fig. 4 for $\mathrm{d}k/\mathrm{d}y = 0$ as wall boundary conditions. The match in both cases with the data is reasonable. In contrast to the hydraulically smooth results (Fig. 2c), the match achieved in the computed k-profiles is particularly impressive (Figs. 3c and 4c). The only significant difference between the two model variants is in the computed k-profiles very near the bed: the use of $k = 0$ forces a steep gradient near

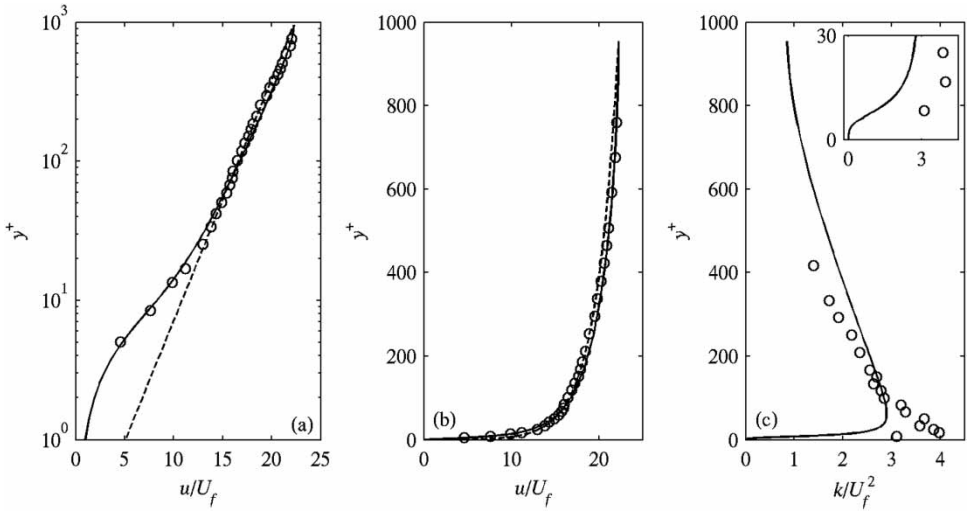

Figure 2 Comparison of (–) computed, (– – –) logarithmic ($u/U_f = (1/\kappa)\cdot \ln(y^+) + 5.1$, $\kappa = 0.40$) and (○) measured (a and b) velocity and (c) turbulent kinetic energy profiles, using the $\mathrm{d}k/\mathrm{d}y = 0$ boundary condition for hydraulically smooth conditions ($\mathsf{R} = 1.9 \times 10^4$, $k_N{}^+ = 1$). Inset in (c) shows k-profile near the bed

the wall, whereas the zero-gradient boundary condition allows for a nearly uniform turbulence profile near the rough wall. Although the measurements are not performed low enough in the column to directly support either model result over the other in this region, the zero-gradient condition for rough walls is, in our opinion, more consistent with the underlying physics, as discussed above. The nearly uniform k values measured for $y/k_N \leq 0.5$ would also seem to generally support this contention (Figs. 3c and 4c).

Although the computed results for the two model variants shown in Figs. 3 and 4 are quite similar, it turns out that the increased physical consistency associated with the $\mathrm{d}k/\mathrm{d}y = 0$ wall boundary condition leads to significant computational advantages for rough walls, which have not been previously demonstrated. This is directly related to the fact that this boundary condition avoids forcing a viscous sublayer in hydraulically rough conditions. To investigate this issue, a series of additional simulations were performed maintaining the number of vertical cells at 100, but where the geometric grid stretching was varied such that the cell height nearest the bed (denoted here as simply Δy) varied considerably. The convergence properties under both model variants will be investigated, expressed as a function of two dimensionless near-wall grid sizes. The first uses the near-wall grid spacing normalized by the traditional viscous length scale, i.e. $\Delta y^+ = \Delta y U_f/\nu$. The second uses the near-wall grid spacing normalized by the roughness length $\Delta y/k_N$, i.e. the natural length scale near hydraulically rough walls. Values of ${k_N}^+ = 200$ as above and ${k_N}^+ = 1000$ were considered, to render any Reynolds number dependence in the convergence properties apparent.

To investigate model convergence, the normalized error of various quantities will be monitored, defined for an arbitrary argument ϕ as

$$\mathrm{Error}\{\phi\} = \frac{\left|\phi_{computed} - \phi_{exact}\right|}{\phi_{exact}} \tag{9}$$

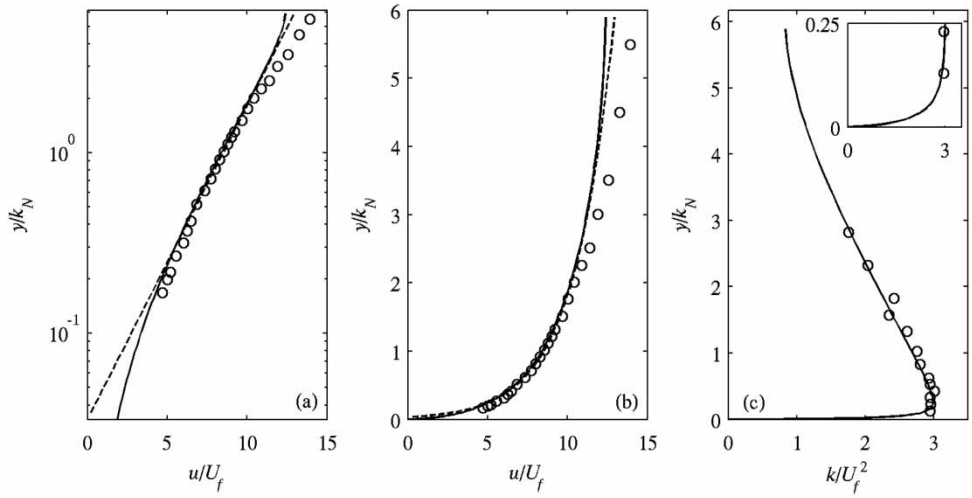

Figure 3 Comparison of (−) computed, (− − −) logarithmic ($u/U_f = 1/\kappa \cdot \ln(30y/k_N)$) and (○) measured (a and b) velocity and (c) turbulent kinetic energy profiles, using the $k = 0$ boundary condition for hydraulically rough conditions (${k_N}^+ = 200$, $\mathsf{R} = 1.4 \times 10^4$). Inset in (c) shows k-profile near bed

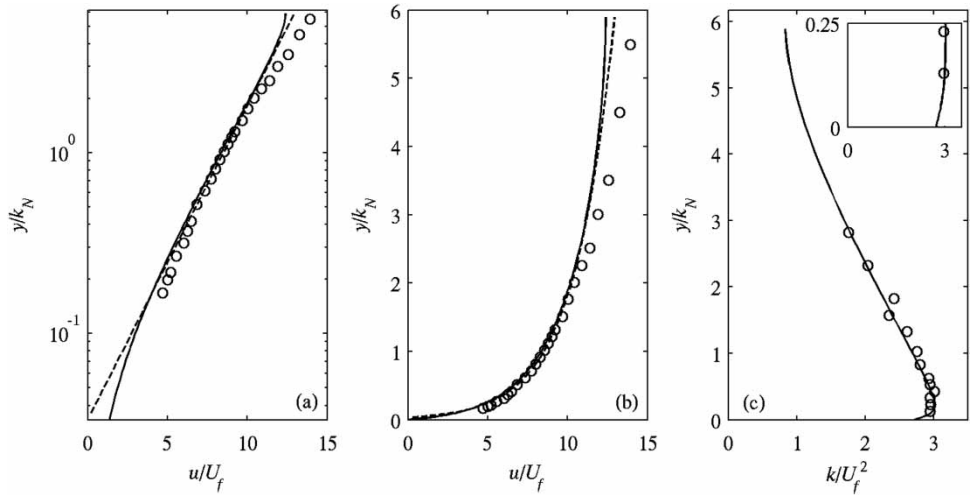

Figure 4 As in Fig. 3, but using a $\mathrm{d}k/\mathrm{d}y = 0$ boundary condition

Here the "exact" results are estimated as those computed with the smallest near-bed grid spacing considered in each series of simulations. To reflect the convergence of the velocity profile, the error of V/U_f will be monitored. Additionally, to reflect the convergence of the near-wall turbulence, the error of k_0/U_f^2 will be monitored if a zero-gradient boundary condition is used, where k_0 is the k-value at the wall, whereas the error of $k_{\max}/U_f^2$ will be monitored if a $k = 0$ wall boundary condition is used.

The resulting error curves are shown in Fig. 5 for simulations using the $k = 0$ wall boundary condition. Clearly, the model convergence properties under this strategy are not governed by either of the parameters alone, as there are four unique curves apparent in both Fig. 5(a) and (b). However, note from Fig. 5(a) that the model only begins to converge as the near-wall grid spacing approximately satisfies $\Delta y^+ \leq 1$. Once this threshold is exceeded, a catastrophic failure occurs, as is evidenced by the sharp increase in the error of $k_{\max}/U_f^2$ for slightly larger grid sizes (Fig. 5a). The error of the mean velocity V/U_f then is erratic. The threshold $\Delta y^+ \leq 1$ is well established for the k-ω model if a $k = 0$ boundary condition is used (e.g. Wilcox 2006), as this condition inevitably necessitates resolution of a viscous sublayer spanning the range $y^+ = yU_f/\nu < 5$. This has a sound physical basis for hydraulically smooth conditions, but is arguably physically inconsistent, and certainly numerically undesirable, for hydraulically rough conditions, as it can require highly-stretched grids to be satisfied. Compounding this problem further is the fact that for large $k_N{}^+$ even more stringent criteria for Δy^+ can be required to achieve grid-independent solutions (e.g. Patel and Yoon 1995, Knopp *et al.* 2009). These findings are generally consistent with the results shown in Fig. 5, as the error for $k_N{}^+ = 200$ is always less than for the equivalently discretized case for $k_N{}^+ = 1000$. When plotted against $\Delta y/k_N$ (Fig. 5b), the respective error curves become more widely separated, indicating that this parameter, while having desired numerical significance on rough beds, unfortunately has little to do with the model convergence properties when the $k = 0$ wall boundary condition is utilized.

The resulting error curves under a $\mathrm{d}k/\mathrm{d}y = 0$ wall boundary condition are similarly shown in Fig. 6. There, no sharp increase in the error is observed in the vicinity of $\Delta y^+ = 1$. This is because a forced viscous sublayer is now avoided entirely for the rough walls considered, as k (and hence ν_T) is allowed to be finite at the wall. When the error is plotted against Δy^+ (Fig. 6a), no consistent trends are observed, hence this quantity no longer seems to play a defining role in the convergence properties, as pure viscous effects are now relatively small throughout the model domain. Alternatively, when plotted against $\Delta y/k_N$ (Fig. 6b), the four error curves from Fig. 6(a) essentially collapse into two, one for the error of each respective quantity V/U_f and k_0/U_f^2. The observed overlay of the curves, with $k_N{}^+$ varying by a factor of 5, convincingly indicates that the model error is now essentially independent of the roughness Reynolds number $k_N{}^+$. This means that the $\mathrm{d}k/\mathrm{d}y = 0$ wall boundary condition allows the near-bed grid spacing for rough walls to be based on the roughness length itself, which is again the natural length scale under hydraulically rough conditions. Note that because $k_N{}^+ = k_N/(\nu/U_f)$ effectively represents the ratio of roughness and viscous length scales, the numerical advantages of the $\mathrm{d}k/\mathrm{d}y = 0$ boundary condition, over the conventional $k = 0$ boundary

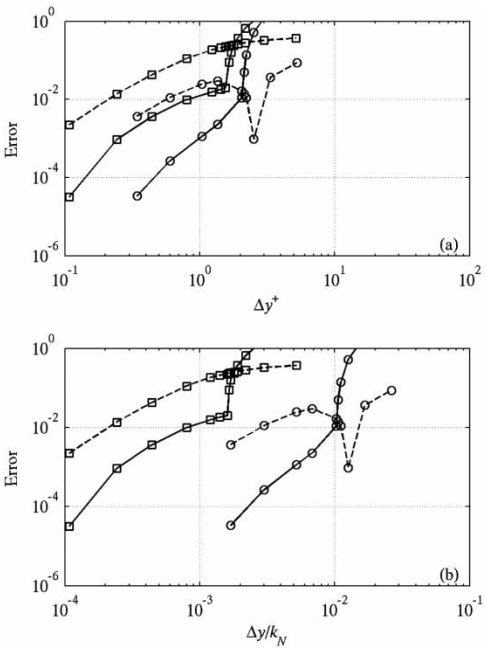

Figure 5 Estimated normalized error of (−) $k_{\max}/U_f^2$ and (− − −) V/U_f from simulations using $k = 0$ wall boundary condition versus (a) Δy^+ and (b) $\Delta y/k_N$. $k_N{}^+$= (○) 200, (□) 1000

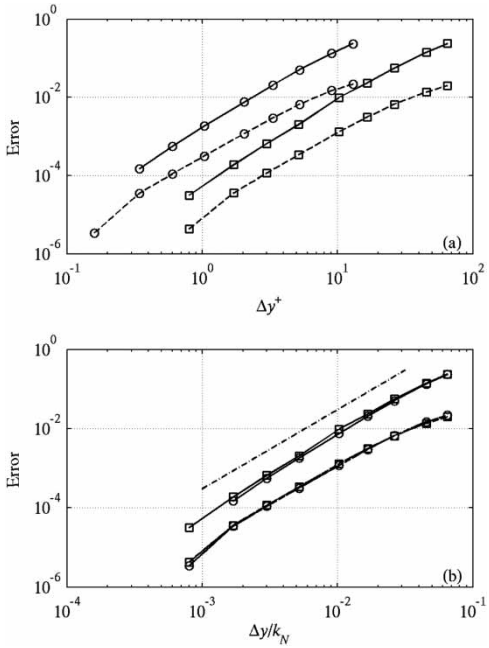

Figure 6 Estimated normalized error of (−) k_0/U_f^2 and (− − −)V/U_f from simulations using the $\mathrm{d}k/\mathrm{d}y = 0$ wall boundary condition versus (a) Δy^+ and (b) $\Delta y/k_N$. $k_N{}^+$= (○) 200, (□) 1000. In (b), (−-−) shows a variation $\sim(\Delta y/k_N)^2$

condition, will become increasingly pronounced as $k_N{}^+$ increases. Based on these results, reasonable accuracy can seemingly be achieved for say $\Delta y/k_N \leq \mathrm{O}(0.01)$.

5 Conclusions

This work compares the use of the conventional $k = 0$ wall-boundary condition for the specific turbulent kinetic energy with an alternative $\mathrm{d}k/\mathrm{d}y = 0$ wall boundary condition, corresponding to zero flux of turbulent kinetic energy through the wall, in conjunction with a two-equation k-ω turbulence model. Comparisons against new experimental measurements for steady open-channel flows demonstrate that accurate results for both mean horizontal velocity and k-profiles, for the bulk of the fluid, can be realized for both hydraulically smooth and rough beds using either condition. The use of the zero-gradient condition, however, offers potentially significant numerical advantages on rough walls. When a smooth wall is considered, the zero-gradient condition naturally allows the formation of a viscous sublayer, which may then be integrated directly, as with a conventional $k = 0$ boundary condition. More importantly, if a rough wall is considered, this condition avoids forcing a fictitious viscous sublayer by allowing finite k at the wall. Hence, this condition is more generally consistent with near-wall physics than the conventionally utilized $k = 0$ wall-boundary condition, which forces a viscous sublayer to be modelled regardless of flow condition and is therefore preferable. Convergence testing indicates that this strategy allows the grid spacing near a rough wall to be based on the roughness length itself, rather than the traditional viscous length scale, alleviating well-known numerical difficulties conventionally associated with the k-ω turbulence model.

Acknowledgements

The authors wish to thank the Danish Center for Scientific Computing for providing computational resources, as well as the Danish Council for Strategic Research (Sea Bed Wind Farm Interaction project, grant no. 2104-07-0010) for financial support. Inspiring discussions with Prof. B. Mutlu Sumer are also acknowledged.

Note

1. OpenFOAM® is a registered trade mark of OpenCFD Limited, the producer of the OpenFOAM software.

Notation

C_{lim} = closure coefficient (–)
d = median grain diameter (L)
h = flow/model depth (L)
k = turbulent kinetic energy per unit mass ($\mathrm{L}^2\mathrm{T}^{-2}$)
k_0 = turbulent kinetic energy per unit mass at bed ($\mathrm{L}^2\mathrm{T}^{-2}$)
k_{max} = maximum turbulent kinetic energy per unit mass along vertical profile ($\mathrm{L}^2\mathrm{T}^{-2}$)
k_N = equivalent sand grain roughness length (L)
$k_N{}^+$ = roughness Reynolds number (–)
p = pressure ($\mathrm{ML}^{-1}\mathrm{T}^{-2}$)
R = Reynolds number (–)
S_{ij} = strain rate tensor (T^{-1})
S_R = function of ω wall boundary condition (–)
t = time (T)
u = horizontal velocity component (LT^{-1})
u_i = Cartesian velocity components (LT^{-1})
u_i' = Cartesian fluctuating velocity components (LT^{-1})
U_f = friction velocity (LT^{-1})
V = depth averaged velocity (LT^{-1})
x = horizontal coordinate (L)
x_i = Cartesian coordinates (L)
y = vertical coordinate (L)
y^+ = vertical wall coordinate (–)
α = closure coefficient (–)
β, β^* = closure coefficients (–)
δ_{ij} = Kronecker delta (–)
κ = von Karman constant (–)
ν = kinematic fluid viscosity ($\mathrm{L}^2\mathrm{T}^{-1}$)
ν_T = kinematic eddy viscosity ($\mathrm{L}^2\mathrm{T}^{-1}$)
ω = specific turbulence dissipation rate (T^{-1})
$\tilde{\omega}$ = limited specific turbulence dissipation rate (T^{-1})
ρ = fluid density (ML^{-3})
σ, σ^* = closure coefficients (–)
σ_d, σ_{do} = closure coefficients (–)
τ_{ij} = Reynolds stress tensor ($\mathrm{L}^2\mathrm{T}^{-2}$)

References

Bayazit, M. (1983). Flow structure and sediment transport mechanics in steep channels. *Euromech* 156*: Mechanics of Sediment Transport*, 197–206, B.M. Summer & A. Muller, eds. Balkema, Rotterdam.

Bayazit, M. (1976). Free surface flow in a channel of large relative roughness. *J. Hydraulic Res*. 14(1), 115–126.

Blinco, R.H., Partheniades, E. (1971). Turbulence characteristics in free surface flows over smooth and rough boundaries. *J. Hydraulic Res*. 9(1), 43–69.

Dixen, M., Hatipoglu, F., Sumer, B.M., Fredsøe, J. (2007). Wave boundary layer over a stone-covered bed. *Coast. Eng*. 55(1), 1–20.

Fuhrman, D.R., Fredsøe, J., Sumer, B.M. (2009). Bed slope effects on turbulent wave boundary layers 1: Model validation and quantification of rough-turbulent results. *J. Geophys. Res*. 114(3), C03024, doi:10.1029/2008JC005045.

Fredsøe, J., Andersen, K.H., Sumer, B.M. (1999). Wave plus current over ripple-covered bed. *Coast. Eng*. 38(4), 177–221.

Hellsten, A., Laine, S. (1998). Extension of *k-ω* shear-stress-transport turbulence model for rough-wall flows. *AIAA J*. 36(9), 1728–1729.

Kamphuis, J.W. (1974). Determination of sand roughness for fixed beds. *J. Hydraulic Res*. 12(2), 193–203.

Knopp, T., Eisfeld, B., Calvo, J.B. (2009). A new extension for *k-ω* turbulence models to account for wall roughness. *Int. J. Heat Fluid Flow* 30(1), 54–65.

Menter, F.R. (1994). Two-equation eddy-viscosity turbulence models for engineering applications. *AIAA J*. 32(8), 1598–1605.

Nezu, I. (1977). Turbulence structures in open-channel flows. *PhD Thesis*. Kyoto University, Kyoto, Japan.

Patel, V.C., Yoon, J.Y. (1995). Application of turbulence models to separated flow over rough surfaces. *J. Fluids Eng*. ASME 117(2), 234–241.

Patel, V.C. (1998). Perspective: Flow at high Reynolds number and over rough surfaces: Achilles heel of CFD. *J. Fluids Eng*. ASME 120(3), 434–444.

Roulund, A., Sumer, B.M., Fredsøe, J., Michelsen, J. (2005). Numerical and experimental investigation of flow and scour around a circular pile. *J. Fluid Mech*. 534, 351–401.

Sana, A., Ghumman, A.-R., Tanaka, H. (2009). Modeling of a rough-wall oscillatory boundary layer using two-equation turbulence models. *J. Hydraulic Eng*. 135(1), 60–65.

Sumer, B.M., Cokgor, S., Fredsøe, J. (2001). Suction removal of sediment from between armour blocks. *J. Hydraulic Eng*. 127(4), 293–306.

Sumer, B.M., Chua, L.H.C., Cheng, N.-S., Fredsøe, J. (2003). Influence of turbulence on bed load sediment transport. *J. Hydraulic Eng*. 129(8), 585–596.

Wilcox, D.C. (2006). *Turbulence modeling for CFD.* 3rd ed. DCW Industries. La Cañada CA.

Wilcox, D.C. (2008). Formulation of the *k-ω* turbulence model revisited. *AIAA J*. 46(11), 2823–2838.